



**AIAA 99–2714**

**Resonance-Probe Measurements of  
Plasma Densities in  
Electric-Propulsion Plumes**

Sven G. Bilén, James M. Haas, Frank S. Gulczinski III,  
and Alec D. Gallimore

*University of Michigan, Ann Arbor, Michigan 48109*

Julia N. Letoutchaia

*Michigan State University, East Lansing, Michigan 48825*

**35th AIAA/ASME/SAE/ASEE Joint Propulsion  
Conference and Exhibit**

**20–24 June 1999**

**Los Angeles, California**

# Resonance-Probe Measurements of Plasma Densities in Electric-Propulsion Plumes

Sven G. Bilén,<sup>\*</sup> James M. Haas,<sup>†</sup> Frank S. Gulczinski III,<sup>‡</sup> and Alec D. Gallimore<sup>§</sup>  
*University of Michigan, Ann Arbor, Michigan 48109*

Julia N. Letoutchaia<sup>¶</sup>  
*Michigan State University, East Lansing, Michigan 48825*

We are developing a resonance-probe plasma diagnostic that uses a microwave network analyzer for use in electric-propulsion research. To show the feasibility of our resonance-probe implementation, we have measured plasma densities in the plume of the 5-kW-class P5 Hall-effect thruster and compared them to measurements made with a Langmuir probe. Our preliminary work in this area indicates that the resonance-probe technique shows considerable promise. The resonance-probe technique should prove to be a useful tool to support electric-propulsion research since it is able to provide high temporal-resolution electron density measurements.

## Nomenclature

$B_0$	background magnetic-flux density, T
$c$	speed of light in a vacuum, $2.998 \times 10^8$ m/s
$k$	Boltzmann's constant, $1.38 \times 10^{-23}$ J/K
$l_{RP}$	resonance-probe tip length, m
$m_e$	electron mass, $9.109 \times 10^{-31}$ kg
$m_i$	ion mass, kg
$n_e$	electron plasma density, $m^{-3}$
$q$	charge magnitude, $1.602 \times 10^{-19}$ C
$T_e$	electron temperature, K
$v_p$	propagation (phase) velocity, m/s
$\epsilon_0$	free space permittivity, $8.85 \times 10^{-12}$ F/m
$\lambda$	wavelength of excitation frequency, m
$\omega_{ce}$	angular electron-cyclotron frequency, rad/s
$\omega_{pe}$	angular electron-plasma frequency, rad/s
$\omega_{uh}$	angular upper-hybrid frequency, rad/s

## Introduction

USING a modern microwave network analyzer, we are developing a resonance-probe (RP) plasma diagnostic for use in electric-propulsion research. To show the feasibility of our RP implementation, we have measured plasma densities in the plume plasma of a Hall-effect thruster. We compare those measurements with those made via the Langmuir probe (LP) technique. Our preliminary work in this area indicates that

the RP technique shows promise and that for some investigations it has several advantages over the Langmuir probe diagnostic.

The resonance probe (also known as the plasma frequency probe or radio frequency impedance probe) technique is used to measure the absolute electron density of a plasma. The typical RP implementation involves immersing an electrically short antenna (probe) in a plasma and determining the frequency at which the antenna reactance is zero.<sup>1</sup> Although the RP technique has been around since the early 1960s, it has seen limited use due to the dominance of the LP plasma diagnostic.

Our RP implementation utilizes a modern network analyzer (NA) attached to the probe itself. There are several benefits to using an NA for researching the RP technique at the prototype stage. First, the NA is extremely flexible and allows the applied probe frequency to be swept over a wide range. This is important since plasma densities, and hence plasma frequencies, may not be known *a priori*. Second, long cable lengths—required of any diagnostic technique placed in a large vacuum chamber—have large losses at microwave frequencies which can be removed via proper system calibration. Third, the time-gating feature of the NA can be used to reduce the effects of signal reflections from the chamber's walls.

In this paper, we will begin with some background on the RP and give a brief overview of its theory of operation. We explain the experimental apparatus used in our experiments, giving particular emphasis to the inclusion of the network analyzer. We then present and discuss our experimental results for measurements in a Hall-thruster plume. We conclude with a summary and give several directions for future work.

<sup>\*</sup>Research Fellow, Radiation Laboratory and Space Physics Research Laboratory, AIAA Member

<sup>†</sup>Graduate Student, Plasmadynamics and Electric Propulsion Laboratory, AIAA Student Member

<sup>‡</sup>Graduate Student, Plasmadynamics and Electric Propulsion Laboratory, AIAA Student Member

<sup>§</sup>Associate Professor, Aerospace Engineering and Applied Physics, AIAA Associate Fellow

<sup>¶</sup>Student, Physics Department

Copyright © 1999 by Sven G. Bilén. Published by the American Institute of Aeronautics and Astronautics, Inc. with permission.

## Resonance Probe Background and Theory

Tonks first used the term “plasma resonance” in the literature in the 1930s.<sup>2,3</sup> He was able to determine that the resonances he measured in the plasma were roughly correlated to the electron plasma frequency. In the early 1960s, interest in the plasma resonance phenomena began again after a set of experiments by Takayama *et al.*<sup>4</sup> indicated that a frequency-swept probe appeared to have a sharp peak at a resonant frequency, which they assumed was the electron plasma frequency. Later work by Levitskii and Shashurin,<sup>5</sup> however, indicated that the peak corresponds to a *series* resonance condition between the sheath and plasma. They found that a *parallel* resonance also occurs at a higher frequency that arises from the resonating between the inductance and capacitance of the plasma. This parallel resonance corresponds to the electron plasma frequency. Harp and Crawford<sup>6</sup> give a review article of the RP in which they also developed a theoretical model to describe the RP behavior and compared it with experimental results. Several other studies<sup>7,8</sup> into the RP’s behavior were subsequently published based on the concept of series and parallel resonances.

An alternative description of the resonance probe begins by realizing that it is actually a short plasma-immersed antenna. In 1964, Balmain<sup>9</sup> developed a theory to calculate the impedance of a short dipole immersed in a magnetoplasma ignoring the sheath. Balmain was able to determine several resonance points corresponding to plasma resonances. Adachi *et al.*<sup>10</sup> included the sheath in their transmission line theory of the antenna impedance. They used a longer antenna and in their analysis found several additional resonance-frequency points, *e.g.*, the upper-hybrid frequency. Their transmission-line analysis generally agreed with Balmain’s analysis as antenna length approaches zero and the sheath is removed.

The RP technique itself is relatively simple in concept. Plasma electrons have a natural resonant frequency known as the electron plasma frequency,  $\omega_{pe}$ , which depends on the plasma density. This frequency, which is also known simply as the plasma frequency,  $\omega_p$ , is given by the equation

$$\omega_p = \omega_{pe} = \sqrt{\frac{n_e q^2}{\epsilon_0 m_e}}. \quad (1)$$

When the RP is immersed in a plasma and driven by an RF sweep frequency, the reactance of the antenna/probe becomes zero at the plasma frequency. Modeling the probe–plasma system as a parallel resonant circuit, this zero reactance frequency occurs where the free space capacitive antenna reactance is cancelled by the inductive reactance of the oscillating electrons.<sup>11</sup>

One of the strengths of this technique lies in the fact that Eqn. 1 can be easily rearranged, yielding plasma density directly when the electron plasma frequency is known, *i.e.*,

$$n_e = \frac{\omega_{pe}^2 \epsilon_0 m_e}{q^2}. \quad (2)$$

Hence, unlike LPs, which rely largely on curve-fitting methods for determining plasma density, RPs can quickly yield a value for plasma density simply by measuring the frequency of resonance. Some RP implementations have yielded  $n_e$  measurements at a rate  $\sim 10$  kHz.<sup>1</sup>

If a magnetic field exists in the plasma, the antenna reactance becomes zero at a frequency slightly higher than the plasma frequency known as the upper hybrid frequency.<sup>1</sup> The upper hybrid frequency is related to the electron plasma and cyclotron frequencies by the relation

$$\omega_{uh}^2 = \omega_{pe}^2 + \omega_{ce}^2, \quad (3)$$

where the electron cyclotron frequency,  $\omega_{ce}$ , is given by the equation

$$\omega_{ce} = \frac{qB_0}{m_e}. \quad (4)$$

Here,  $B_0$  is an external magnetic field such as that of the thruster or of the Earth. If the magnetic field is known and static (as it would be near a plasma electric thruster), then this increase in resonant frequency does not complicate the analysis significantly.

## Experimental Apparatus

### Vacuum Chamber Description

The University of Michigan’s Plasmadynamics and Electric Propulsion Laboratory (PEPL) has as its centerpiece the Large Vacuum Test Facility (LVTF), a cylindrical, stainless-steel-clad tank which is 9 m long and 6 m in diameter.<sup>12</sup> The facility has four nude cryopumps backed by two 2000 cfm (56,600 l/s) blowers and four 400 cfm (11,300 l/s) mechanical pumps. These pumps give the facility a combined pumping speed of 300,000 l/s on air and 140,000 l/s on xenon and provide the ability to reach a high vacuum ( $10^{-7}$  torr). Fig. 1 is a diagram of the LVTF as it was set up for the resonance-probe measurements of the P5 thruster described below.

### P5 Thruster Description

The PEPL 5-kW-class Hall-effect thruster—dubbed the P5—was jointly developed by the University of Michigan and the United States Air Force Research Laboratory to support research into the basic physics of Hall-effect thrusters.<sup>13</sup> The P5 is well suited for diagnostic access, particularly internal diagnostic access, and is easily modifiable such that the effects of changes in thruster configuration can be examined. Fig. 2 shows the P5 as set up for the RP characterization. For these experiments, the thruster was run on xenon propellant ( $m_i = 2.18 \times 10^{-25}$  kg).

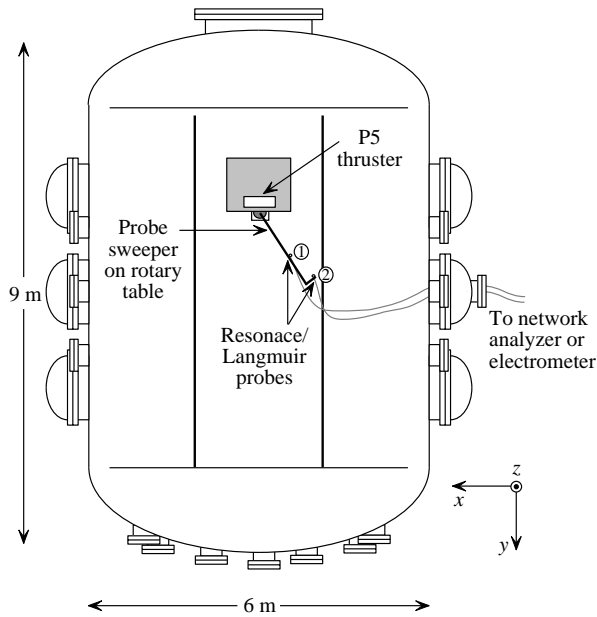


Fig. 1 Setup of the vacuum chamber for the resonance probe measurements of the P5.

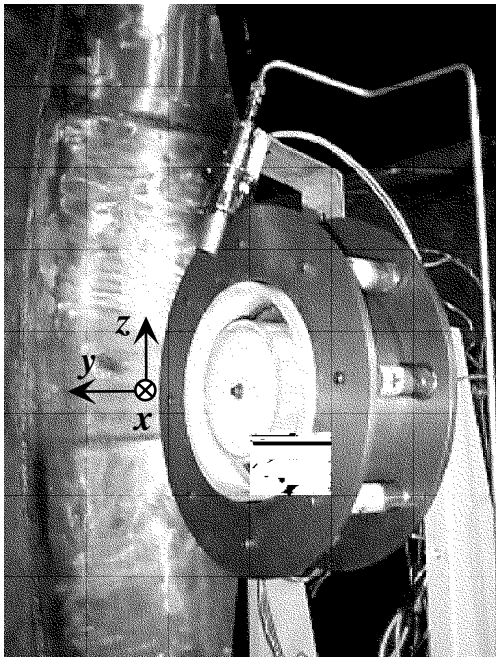


Fig. 2 Picture of the P5 (axis orientation shown in this figure corresponds to that of Fig. 1).

## Measurement Equipment

The measurement equipment used during these experiments included a network analyzer, electrometer, computer controller, and a rotary table. The network analyzer and electrometer were connected via an IEEE-488 bus to the computer controller, which set equipment parameters, controlled instruments, and stored data. A more detailed description of the equipment used and their function is listed below.

**Network Analyzer** A Hewlett-Packard 8753D network analyzer was used to drive the resonance probes with RF energy. The NA can sweep from 30 kHz to 6 GHz, contains an integrated S-parameter test set, has a 105-dB dynamic range, and has the capability of time-domain measurements.

**Electrometer** A Keithley 2410 Source Electrometer was used to drive the Langmuir probe (LP) system. The electrometer measured the current collected by the LP as it was swept from  $-20$  to  $+80$  V. LP measurements were used to determine electron temperatures and number densities in the P5 plasma plume.

**Computer Controller** An Apple Macintosh Quadra running LabVIEW software from National Instruments was used to set equipment parameters and to store data via an IEEE-488 bus. LabVIEW routines were used to control the network analyzer and to drive the electrometer and capture LP traces.

**Rotary Table** A rotary table, developed by New England Affiliated Technologies (NEAT), was used to sweep (in a  $\theta$ -directed arc) the RP/LP's through the P5's plasma plume.

Fig. 3 shows how the equipment was electrically connected for the RP measurements. The RP and LP were physically the same probe; therefore, to make LP measurements the cable was removed from the NA and attached to the electrometer.

## Probe Description and Mounting

The construction of the resonance probe itself is rather simple and is shown in Fig. 4. The probe consists of a piece of semi-rigid microwave coaxial cable that has been stripped of its shield and dielectric on one end to form the RP tip. The tip was ground down such that there were no sharp corners that would cause fringing fields and its length was electrically short (*i.e.*,  $l_{RP} < \lambda/20$ ) at the frequencies of interest. The specific cable used for our initial implementation is Precision Tube's AA50141, which is a  $50\text{-}\Omega$  cable with a silvered copper-covered steel wire as center conductor, a polytetrafluoroethylene (PTFE) dielectric, and a copper outer conductor. The semi-rigid tubing is connected

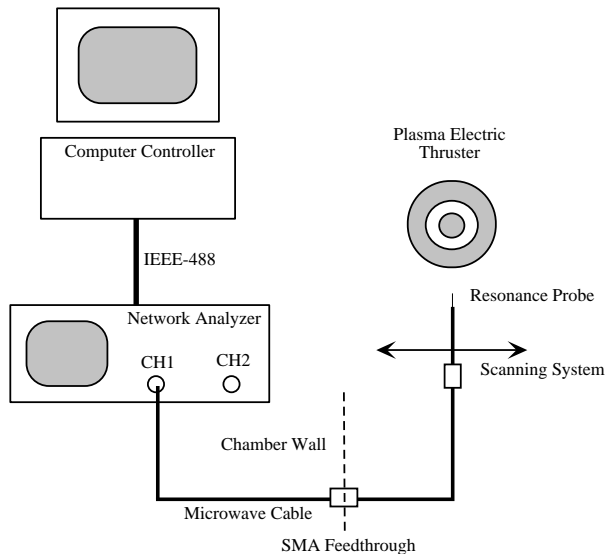


Fig. 3 Schematic of the experimental setup.

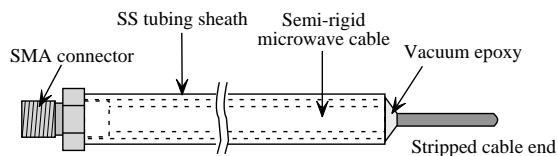


Fig. 4 Diagram of the construction of the resonance probe.

to a female SMA connector. A stainless-steel (SS) tube sheath is placed around the semi-rigid cable for added protection and vacuum epoxy is used to seal in the PTFE dielectric.

The probes were mounted to a sweeper mast attached to the rotary platform, which itself was located directly beneath the P5 thruster such that the mast's pivot point was in the plane of the thruster. RP/LP-1 was located along the thruster centerline at a distance of 70 cm; RP/LP-2 was located 8 cm to the left of the centerline at a distance of 110 cm (see Fig. 1). RP/LP-2 was offset so that possible shadowing by RP/LP-1 would be minimized. The probes were mounted at a height such that they were aligned with the thruster's center. The sweeper mast could rotate under computer control from  $-60^\circ \leq \theta \leq +60^\circ$ . Fig. 5 shows a picture of the experimental configuration.

#### Network Analyzer System Setup and Calibration

When making measurements at microwave frequencies, it is extremely important to remove cabling and connector losses via calibration. This is especially important when working with the long cable lengths required of any diagnostic placed in a large vacuum chamber like the LVTF. For our experiments, we used QMI, Inc.'s "Workhorse" series microwave cables, which have high phase stability, a cable loss of  $< 35$

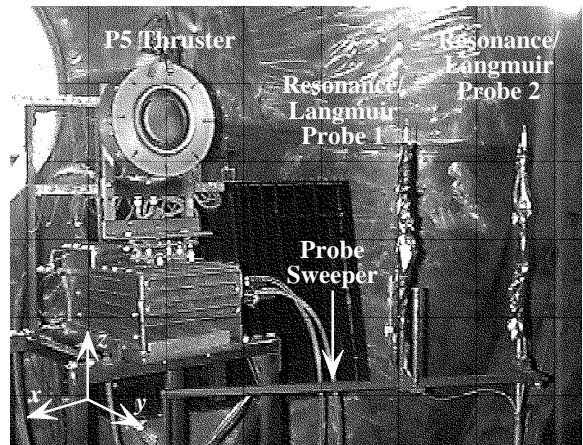


Fig. 5 Picture of the experimental setup for the resonance probe characterization of the P5 thruster.

dB/100 ft. (1.14 dB/m), and a velocity of propagation  $v_p = 0.707c$ . To reach the outside of the chamber, the cable lengths were 30 ft. (9.14 m) each, which introduced considerable loss and phase delay. Additional losses occurred at the SMA vacuum feedthroughs and the probes' SMA connectors.

To remove as much of these effects as possible, we performed a single port (*i.e.*,  $S_{11}$ , a measurement of reflected energy) calibration of the NA using an HP 85033D calibration kit. Since we required that the reference plane of the measurements be at the RP tip itself, we first placed a "dummy" section of semi-rigid cable at the end of the 30-ft. microwave cables to take the place of the RP's cable length (*i.e.*, everything but the tip). The NA was then calibrated using the required short, open, and 50- $\Omega$  loads from the calibration kit. Using the time-domain capability of the NA, we then determined the phase length from the NA to the RP tip by identifying the distance to the largest mismatch, *i.e.*, the "open" of the RP tip. The NA subtracted this electrical length from all measurements. With this procedure, we were able to make measurements approximately as if the only piece in the overall system were the RP tip itself.

The NA was set up such that it collected 801 points per sweep with a smoothing window of 1%. Output power was 0 dBm (1 mW). Each sweep covered the frequency range from 1 MHz to 1 GHz; hence the frequency resolution was 1.25 MHz.

### Experimental Results

The P5 thruster was run at 5 different operating conditions roughly providing 5 different plasma plume densities (Table 1). At each operating condition, the RP/LPs were swept twice through the plume. During the first sweep LP data was collected; the second sweep collected RP data.

We show here the same collected RP data (data is

**Table 1 Summary of operating conditions for the P5 thruster.**

Oper. Cond.	Flowrate, sccm	Discharge Voltage, V	Discharge Current, A
1	65.7	200	5.2
2	65.7	300	5.1
3	115.0	500	10.0
4	154.5	300	15.1
5	65.4	300	5.3

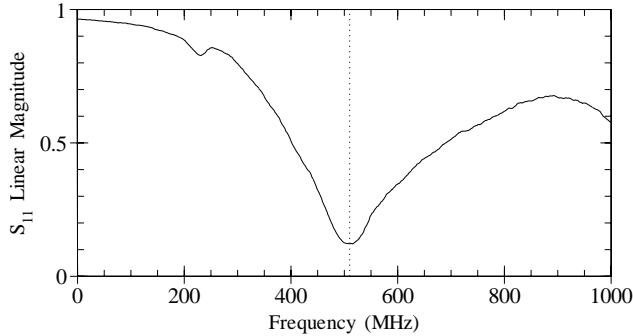


**Fig. 6 Sample resonance-probe data (RP/LP-1, P5 cond. 4, 0° radial angle) showing linear magnitude of  $S_{11}$ . Minimum occurs at ~510 MHz.**

from RP/LP-1, cond. 4, 0° radial angle) plotted in two different manners, which corresponds to the two complementary descriptions given for RP response (see section on RP theory). Fig. 6 plots the linear magnitude of the  $S_{11}$  component where it is seen that a minimum in the response occurs at ~510 MHz. This minimum occurs at the parallel resonance.

Fig. 7 plots the same data on a Smith chart. Smith charts are useful for examining complex impedance data in a visual manner.\* Real impedances lie along the center line, whereas reactances lie above and below the center line. The top half of the chart corresponds to inductive reactances and the bottom half corresponds to capacitive reactances. Here we see that the impedance of the probe/antenna is initially in the top half indicating that it is inductive; at 493 MHz, the impedance becomes capacitive. This is as expected since at resonance the free-space capacitive antenna reactance is cancelled by the inductive reactance of the oscillating electrons.

After determining the resonance-frequency values, plasma density is determined via Eqn. 2. For the results here we have ignored any magnetic fields; hence  $\omega_{ce} \rightarrow 0$ . Comparisons of LP- and RP-derived plasma densities are shown in Figs. 8-12.

## Discussion

These data presented here for electron densities in the plume of the P5 thruster agree well with those col-

\*See Pozar,<sup>14</sup> Section 3.4 for a more detailed description of the Smith chart and its use.

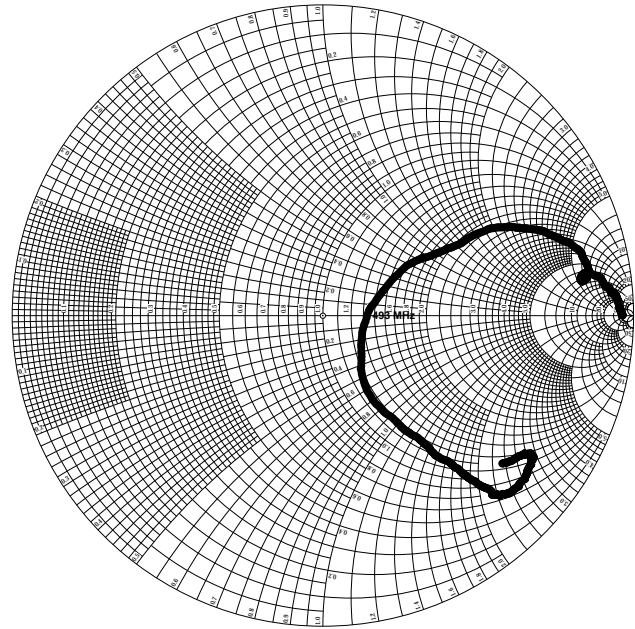


**Fig. 7 Sample resonance-probe data (RP/LP-1, P5 cond. 4, 0° radial angle) plotted on a Smith chart. Resonance occurs at crossover point ~493 MHz.**

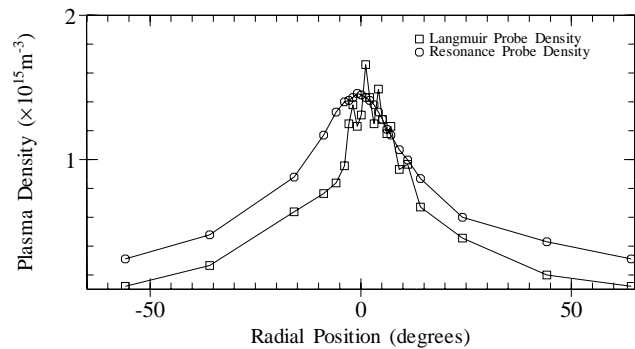


**Fig. 8 Comparison of plasma densities derived from the Langmuir probe and resonance probe techniques (RP/LP-2, P5 cond. 1).**

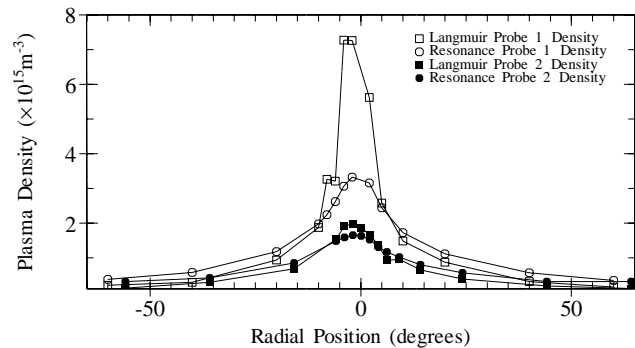


**Fig. 9 Comparison of plasma densities derived from the Langmuir probe and resonance probe techniques (RP/LP-1 & 2, P5 cond. 2).**

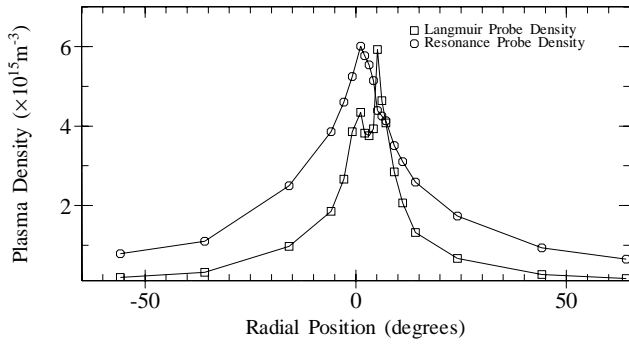


Fig. 10 Comparison of plasma densities derived from the Langmuir probe and resonance probe techniques (RP/LP-2, P5 cond. 3).

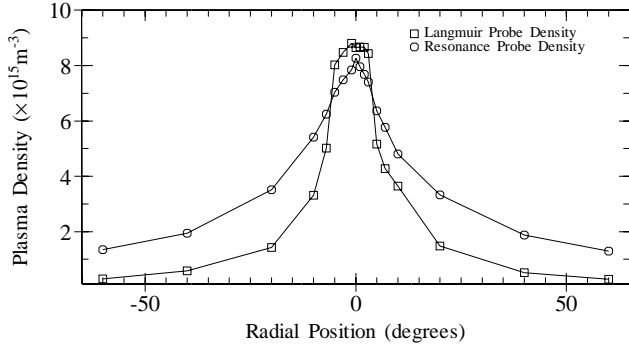


Fig. 11 Comparison of plasma densities derived from the Langmuir probe and resonance probe techniques (RP/LP-1, P5 cond. 4).

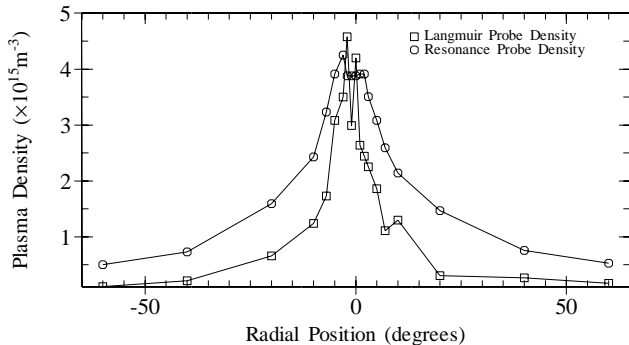


Fig. 12 Comparison of plasma densities derived from the Langmuir probe and resonance probe techniques (RP/LP-1, P5 cond. 5).

lected by Haas *et al.*<sup>13</sup> Figs. 8–12 plot the LP- and RP-derived plasma densities. We see that in all plots, the qualitative agreement is good and the quantitative agreement is generally within the error of the LP technique ( $\sim \pm 50\%$ ).

At some point during the tests (possibly around Cond. 3), the PTFE dielectric of the shorter RP/LP-2 began to extrude due to the heat build-up of the plume impinging on the probes. After sufficient pressure built up, the expanding PTFE broke the vacuum epoxy and migrated along the RP tip where some of it “burned” away. This event made correlations between LP and RP data impossible for this probe later in the test.

This PTFE extrusion did not occur with the longer RP/LP-1, although it was closer and should have experienced more heating. We feel that the increased length kept the expanding PTFE from building up enough pressure to break the vacuum epoxy seal; hence the PTFE remained contained.

### Sources of Error

There are several sources of error for the RP technique. The first is based on the assumption that the correct resonance peak is being investigated. Since the plasma contains resonances besides the electron plasma resonance, care must be made that the correct peak is being examined (note the presence of a second smaller peak in Fig. 6.) Another source of error, as alluded to above, is the system loss due to the long cable lengths, which can cause broadening of the peaks. Although the system was calibrated, movement of the cables when sweeping the probes can cause changes in response that cannot be removed. Since the RP measurement is sensitive to changes in phase,<sup>†</sup> movement and heating due to plume impingement can cause the total phase lag to vary over time. Finally, frequency resolution corresponds directly to plasma density; *e.g.*, in our case, the 1.25-MHz frequency sweep resolution corresponds to  $n_e \pm 2 \times 10^{10} \text{ m}^{-3}$ .

### System Improvements

In this initial RP implementation, the use of a NA to make the measurements provided us with several benefits. However, as a dedicated diagnostic such an implementation is impracticable. NAs are generally very expensive because they contain a lot of circuitry that is not needed for the RP application. Hence, to move to a turn-key diagnostic, an RP implementation much like that of Jensen and Baker<sup>1</sup> should be made. Although designed for the ionosphere, their system consisted of a phase-locked loop which tracked the frequency where antenna reactance was zero. This would make the system much faster and able to be located within the chamber, significantly shortening the line-lengths to the probe, one of the largest contributors to system error.

One possible way to overcome the heat-induced PTFE-extrusion problem is to use a semi-rigid cable that has  $\text{SiO}_2$  as its dielectric.<sup>‡</sup> This would extend the maximum temperature range of the cable from  $\sim 200 \text{ }^\circ\text{C}$  to  $\gtrsim 600 \text{ }^\circ\text{C}$ . Use of  $\text{SiO}_2$  dielectric has the added benefit of providing much better phase stability over the entire temperature range of operation.

One possible implementation of the RP is as an internal diagnostic of an electric-propulsion thruster. Because the probes can be arbitrarily shaped, they can

<sup>†</sup>Recall that the reactive component, related to phase, goes from inductive to capacitive at resonance.

<sup>‡</sup>We recently discovered that Kaman Instrumentation manufactures a semi-flexible  $\text{SiO}_2$  cable, which may prove successful for our RP application.

be placed inside the thruster, or could possibly even be pieces of the thruster itself into which RF energy could be coupled. Similar implementations using electrostatic probes have been made on other thrusters.<sup>15</sup>

This probe possibly can be used to measure other resonances such as ion resonances.<sup>16</sup> It also could be possible to extract other plasma characteristics, such as collision frequency, from the quality factor (the width) of the resonance peak. Also, as in this implementation, a combination resonance/Langmuir probe could be implemented in which the relative strengths of each method would complement each other, *i.e.*,  $n_e$  measurements by the RP and  $T_e$  by the LP.

## Summary

We have implemented a plasma resonance-probe plasma diagnostic with a microwave network analyzer. The strength in utilizing an NA is that we can quickly try different RF drive and collection parameters, which is important since our implementation is a work in progress. We used the RP to determine plasma densities in the plume of the P5 Hall-effect thruster and compared those to LP-derived values.

Our preliminary work indicates that the RP technique shows promise and that it should prove to be a useful tool to support electric-propulsion research. The resonance-probe technique can be used to complement the Langmuir probe technique and it might be possible to extract other important plasma characteristics, such as collision frequency.

## Acknowledgments

This research was funded in part by a Michigan Space Grant Consortium Research Seed Grant. One of the authors (J.N.L.) was supported under the National Science Foundation's Research Experience for Undergraduates (REU) program. The authors wish to thank S. G. Ohler and J. Mahowald for help with previous RP experiments and the PEPL research group for help in performing these experiments. J. M. Haas and F. S. Gulczinski are supported by the United States Air Force Palace Knight Program.

## References

- <sup>1</sup>Jensen, M. D., and Baker, K. D., "Measuring Ionospheric Electron Density Using the Plasma Frequency Probe," *Journal of Spacecraft and Rockets*, Vol. 29, No. 1, 1992, pp. 91–95.
- <sup>2</sup>Tonks, L., "The High Frequency Behavior of a Plasma," *Physical Review*, Vol. 37, 1931, pp. 1458–1483.
- <sup>3</sup>Tonks, L., "Plasma-Electron Resonance, Plasma Resonance and Plasma Shape," *Physical Review*, Vol. 38, 1931, pp. 1219–1223.
- <sup>4</sup>Takayama, K., Ikegami, H., and Miyazaki, S., "Plasma Resonance in a Radio-Frequency Probe," *Physical Review Letters*, Vol. 5, 1960, pp. 238–240.
- <sup>5</sup>Levitskii, S. M., and Shashurin, I. P., "Transmission of a Signal Between Two High-Frequency Probes in a Plasma," *Soviet Physics—Technical Physics*, Vol. 8, 1963, pp. 319–324.

<sup>6</sup>Harp, R. S., and Crawford, F. W., "Characteristics of the Plasma Resonance Probe," *Journal of Applied Physics*, Vol. 35, 1964, pp. 3436–3446.

<sup>7</sup>Dote, T., and Ichimiya, T., "Characteristics of Resonance Probes," *Journal of Applied Physics*, Vol. 36, 1965, pp. 1866–1872.

<sup>8</sup>Ikezi, H., and Takayama, T., "Resonances of Radio Frequency Probe in a Plasma," *Journal of the Physical Society of Japan*, Vol. 21, 1966, pp. 2021–2028.

<sup>9</sup>Balmain, K. G., "The Impedance of a Short Dipole Antenna in a Magnetoplasma," *IEEE Transactions on Antennas and Propagation*, Vol. AP-12, 1964, pp. 605–617.

<sup>10</sup>Adachi, S., Ishizone, T., and Mushiaki, Y., "Transmission Line Theory of Antenna Impedance in a Magnetosphere," *Radio Science*, Vol. 12, 1977, pp. 23–31.

<sup>11</sup>Swenson, C. M., "An Evaluation of the Plasma Frequency Probe," M.S. thesis, Utah State Univ., 1989.

<sup>12</sup>Gallimore, A. D., Kim, S.-W., Foster, J. E., King, L. B., and Gulczinski III, F. S., "Near and Far Field Plume Studies of a One-Kilowatt Arcjet," *AIAA J. Prop. Power*, Vol. 12, 1996, pp. 105–111.

<sup>13</sup>Haas, James M., Gulczinski III, Frank S., Gallimore, Alec D., Spanjers, Gregory G., and Spores, Ronald A., "Performance Characteristics of a 5 kW Laboratory Hall Thruster," *AIAA Paper AIAA-98-3503*, 1998.

<sup>14</sup>Pozar, D. M., *Microwave Engineering*, Addison-Wesley, New York, 1990.

<sup>15</sup>Tiliakos, N. T., Burton, R. L., and Krier, H., "Arcjet Anode Plasma Measurements Using Electrostatic Probes," *AIAA J. Prop. Power*, Vol. 14, No. 4, 1998, pp. 560–567.

<sup>16</sup>Kato, K., Ogawa, K., Yoseli, M., and Shimahara, H., "Observations of the Ion Resonance by a rf Probe," *Journal of the Physical Society of Japan*, Vol. 18, 1963, pp. 1849–1850.